Divergent Synthesis of Complex *ent*-Kauranes, *ent*-Atisanes and *ent*-Trachylobanes via a Hybrid Oxidative Approach

Xiao Zhang, Emma King-Smith, Liao-Bin Dong, Li-Cheng Yang, Jeffrey D. Rudolf, Ben Shen, Hans Renata*

Department of Chemistry, The Scripps Research Institute, 130 Scripps Way, Jupiter, FL 33458
*Correspondence to: hrenata@scripps.edu

Abstract:
The *ent*-kauranes, *ent*-atisanes and *ent*-trachylobanes are large families of complex diterpenes (>1000 members) that exhibit many important biological activities, including inhibition of ion channels, signal transduction cascades and the inflammasome. Due to their structural complexity, *de novo* synthetic access to these molecules are still highly challenging and semisynthetic access has been limited by the lack of chemical tools for scaffold modifications. Here, we report a chemoenzymatic platform to access highly oxidized *ent*-kauranes, *ent*-atisanes and *ent*-trachylobanes via a hybrid oxidative approach that strategically combines chemical and enzymatic oxidation methods. This approach allows selective oxidations of previously inaccessible sites on the parent carbocycles and enables abiotic skeletal rearrangements to the more elusive *ent*-atisane and *ent*-trachylobane architectures. Using this approach, a total of nine complex natural products with rich oxygenation patterns and skeletal diversity were each synthesized in ten steps or less from *ent*-steviol. This work lays the foundation for rapid access to these complex natural products to enable further biological investigations and should inspire continued innovations in exploiting biocatalysis for natural product synthesis.

Introduction

The *ent*-kauranes, *ent*-atisanes and *ent*-trachylobanes (Figure 1A) are biosynthetically-related families of diterpene natural products with wide-ranging biological activities.[1] Members of the *ent*-kaurane family have been reported to exhibit a variety of inhibitory activities, including Skp2 downregulation,[2] Hsp90 inhibition[3] and NLRP3 inhibition.[4] Conversely, atisane-type diterpene alkaloids are noted for their ability to modulate Na^+ and/or K^+ ion channels.[5] Several oxidized *ent*-atisanes, such as a ketone derivative of the spiramilactones (e.g. **5**), have also been reported to display anti-inflammatory activities and inhibition of Wnt/catenin signaling pathway.[6] Though not as common, several bioactive *ent*-trachylobanes have been isolated including the mitrephorones (e.g. **7**, **8**), three highly oxidized *ent*-trachylobanes with moderate cytotoxicity against epidermoid carcinoma cells.[7] The main structural difference between the three natural product families lies in the carbocyclic architecture of their C/D rings: *ent*-kauranes share a common [3.2.1] bicyclic ring system while *ent*-atisanes and *ent*-trachylobanes are characterized by the presence of a [2.2.2] bicycle and [3.2.1.0] tricycle, respectively. These three distinct ring systems are thought to arise from a common precursor,[8] *ent*-copalyl pyrophosphate, through several Wagner–Meerwein shifts following initial formation of *ent*-pimarenyl cation. Oxidative tailoring and oxidation-enabled rearrangements could then take place on the minimally-oxidized carbocyclic skeleton, contributing to the enormous diversity found in the three natural product families. With a few exceptions,[9] little is known about *ent*-atisane and *ent*-trachylobane synthases and most of the oxygenases that are

responsible for the subsequent tailoring events have yet to be identified. Such limitations have rendered synthetic biology access to these privileged structures difficult.

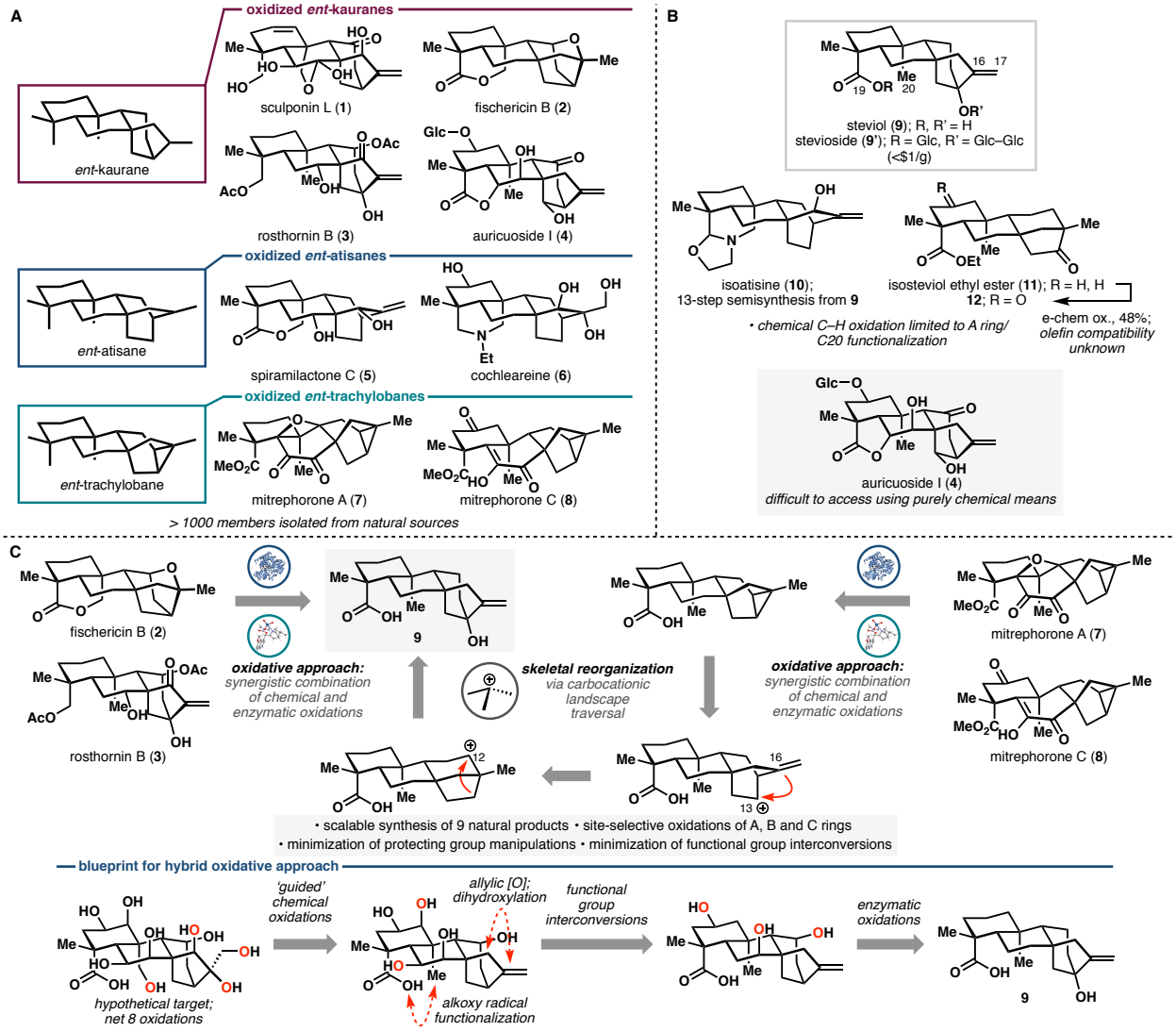

Figure 1. A. Selected examples of oxidized *ent*-kauranes, *ent*-atisanes and *ent*-trachylobanes. **B.** Limitations of purely chemical C–H oxidation approaches in steviol-based semisynthesis. **C.** Retrosynthetic analysis of oxidized *ent*-kauranes, *ent*-atisanes and *ent*-trachylobanes employing a hybrid oxidative approach that combines chemical and enzymatic C–H oxidations.

Due to their intriguing architectures and promising biological activities, *ent*-kauranes, *ent*-atisanes, and *ent*-trachylobanes have been the subject of many synthetic studies, more commonly through the use of *de novo* approaches[10,11,12,13,14] (see Figure S1 for full detail). Semisynthetic efforts, while not as popular, have also been pursued, including Mander's pioneering synthesis of 6,7-*seco*-*ent*-kauranes from gibberellic acid[15] and recent syntheses[16,17] of atisane-type diterpene alkaloids (e.g. **10**, Figure 1B) and neotripterifordin from stevioside. These examples suggest the possibility of developing a more systematic pursuit of highly oxidized *ent*-kauranes from stevioside, which at $0.65/g, represents an attractive starting point for synthesis. However, the realization of this concept has been hampered by the lack of useful methods for scaffold modification. As steviol (stevioside aglycone, **9**) lacks any appropriate functional handles within

its A, B or C ring, semisynthetic elaborations of the framework have mostly relied on the use of C19 functionality in Hofmann–Löffler–Freytag or Suarez hypoiodite reactions[16,17], which currently only allow modification of the C20 methyl group. Remote chemical oxidation of steviol has remained unexplored, likely due to the incompatibility of its C16–C17 *exo* olefin with C–H oxidation conditions. To the best of our knowledge, such oxidation has only been performed electrochemically[18] on isosteviol ethyl ester (**11**), an *ent*-beyerane compound lacking any olefin, producing the corresponding C2-keto product. To date, there is no known chemical method that can effect efficient remote, site-selective C–H functionalization of *ent*-kaurane skeleton, which represents a roadblock in converting steviol to *ent*-kauranes containing multiple oxidations on their A, B and/or C rings (e.g. auricuoside I, Figure 1B). Furthermore, oxidized *ent*-atisanes and *ent*-trachylobanes remain hard to access using semisynthetic approaches as no methods are currently available to convert the C/D ring of *ent*-kaurane to those of *ent*-atisane and *ent*-trachylobane in a facile manner (< five steps).

Here, we report the development of a chemoenzymatic synthetic strategy to access a wide array of oxidized *ent*-kauranes, *ent*-atisanes and *ent*-trachylobanes. Unique within this strategy is the application of a hybrid oxidative approach featuring a combination of remote biocatalytic hydroxylations and 'guided' C–H oxidation methods[19] to access to a variety of oxidation patterns previously unattainable using purely chemical means. In prior applications of C–H functionalization in natural product synthesis, each of these oxidation strategies has only been employed independently,[20,21] but never combined in a synergistic fashion. Our strategy also facilitates the design of a skeletal reorganization sequence towards *ent*-atisane and *ent*-trachylobane frameworks starting from steviol (Figure 1C), which can be combined with an analogous oxidation series to afford highly decorated members of the families. A total of nine natural product targets were synthesized with high synthetic ideality, as well as redox- and step-economy, highlighting the enabling nature of our strategy.

Enzymatic Tool Development for Scaffold Modifications

The overarching premise of our synthetic strategy is to identify biocatalytic oxidation methods to address the methodology gap in the selective functionalization of the A, B and C rings of minimally oxidized *ent*-kaurane, *ent*-atisane and *ent*-trachylobane skeletons. Here, each of the newly introduced hydroxyl group is viewed as a gateway for further manipulations to access many members of these diterpene families through a combination of functional group interconversions and chemical C–H oxidation methods as illustrated in Figure 1C. To access the *ent*-atisane and *ent*-trachylobane frameworks, we drew inspiration from the postulated biogenetic relationship between the two and the *ent*-kaurane framework. One hypothesis[8] proposed that they arise from a common *ent*-beyeranyl carbocation via divergent alkyl/H shifts. As such rearrangements could potentially be reversible in nature, we hypothesized that under suitable conditions, an *ent*-beyerane skeleton could be converted to an *ent*-atisane or *ent*-trachylobane product. Synthetic entry into this sequence could be achieved readily via the well-precedented conversion of the *ent*-kaurene stevioside to the *ent*-beyerane isosteviol. We postulated that further carbocation generation at C12 would trigger a Wagner–Meerwein rearrangement to an *ent*-atisane product, from which access to the *ent*-trachylobane framework could be realized via C–C bond formation between C13 and C16. Following such skeletal reorganization,[22] an array of oxidative transformations on minimally-oxidized *ent*-atisane and *ent*-trachylobane skeleton would provide rapid access to targets such as spiramilactone C (**5**) and the mitrephorones (**7**, **8**).

Successful execution of the aforementioned strategy would thus hinge on the identification of the appropriate enzymes for selective and practical oxidations of the A, B and C rings of steviol. Prior investigations in this area have not resulted in the development of synthetically-useful methods (Figure 2A, 2B). The C7 hydroxylase from gibberellin biosynthesis[23,24] catalyzes further oxidation at C6 and subsequent B ring rearrangement to generate GA_{12}-aldehyde (**14**) and whole-cell fungal biotransformations[25] typically lead to non-selective C–H oxidation, likely due to the involvement of multiple promiscuous enzymes in the cells. In contrast, recent characterization of the platensimycin biosynthesis pathway has revealed the presence of several dedicated *ent*-kaurane hydroxylases for selective C–H oxidations.[26,27] Early in the pathway, a P450 monooxygenase, PtmO5, catalyzes a remote C–H hydroxylation at the C11 position of *ent*-kauranol, followed by an intramolecular cyclization to form the ether bridge. Next, two functionally-redundant α-ketoglutarate-dependent dioxygenases (Fe/αKGs), PtmO3 and PtmO6, hydroxylate the C7 carbon from the β face *en route* to the construction of the enone functionality of platensimycin. We hypothesized that if these enzymes possess sufficient substrate promiscuity to accept steviol or *ent*-kaurenoic acid as substrate, and could do so with high reaction efficiency, they would comprise ideal biocatalysts for use in our synthetic campaign. We began testing this hypothesis by investigating the synthetic utility of PtmO3 and PtmO6 for the oxidation of **9** and **13**. While PtmO3 and PtmO6 are highly homologous (99% identical), the latter was better overproduced upon expression in *E. coli*. Thus, PtmO6 was employed exclusively in this investigation. Gratifyingly, selective C7 hydroxylation of **9** and **13** could be observed with high total turnover numbers (TTN = 1,200 and 390 respectively, Figure 2C), suggesting the utility of this enzyme for preparative-scale B ring oxidation of *ent*-kauranes.

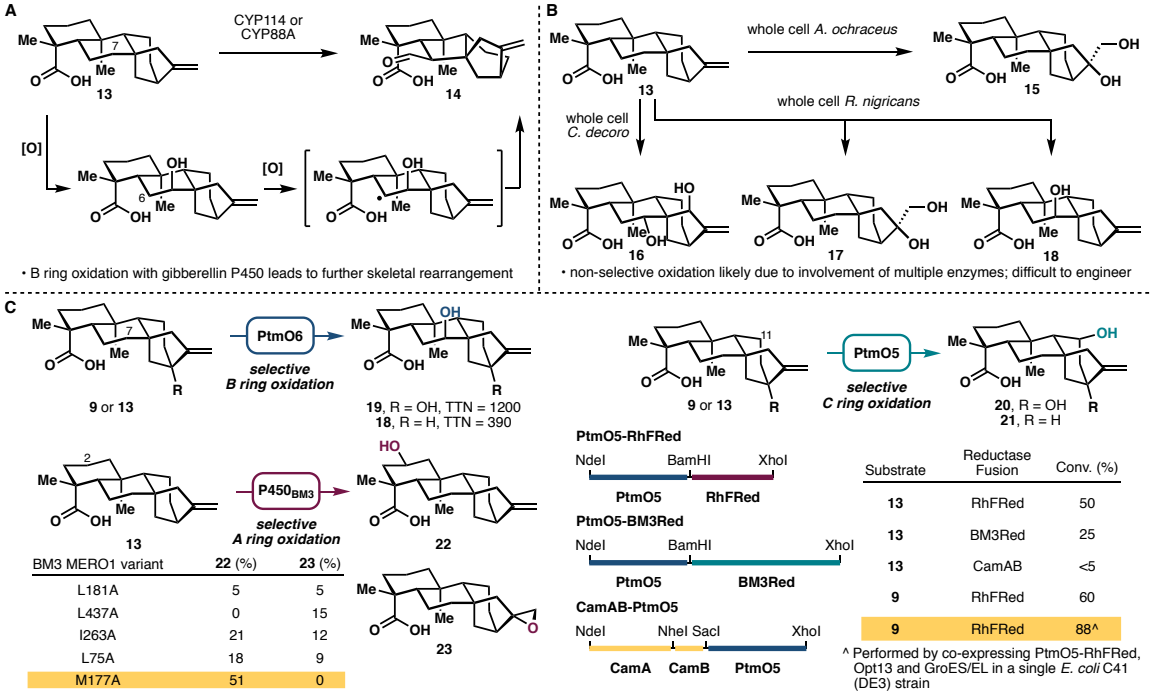

Figure 2. A. The involvement of oxygenases in the conversion of *ent*-kaurenoic acid (**13**) to a gibberellane product. **B.** Non-selective oxidation of **9** using whole-cell fungal biotransformation. **C.** Discovery of three enzymes, PtmO6, PtmO5-RhFRed and BM3 MERO1 M177A for site-selective oxidations at C7, C11, and C2 respectively. See Supporting Information for reaction conditions.

As no P450 reductase could be found in the platensimycin biosynthetic gene cluster, we have previously employed the CamA/B reductase system for the functional characterization of PtmO5.[26] However, the need for separate expression of CamA/B limits the practical use of this system. In contrast, artificial fusion with a reductase partner allows the generation of self-sufficient biocatalyst and bypasses the need for parallel enzyme production.[28,29] This strategy has also been observed to improve electron transfer and reaction coupling efficiency. Based on these perceived advantages, we generated several chimeras of PtmO5 containing artificial fusion with known reductase domains[29,30] and tested their catalytic activity in crude lysates. Among the chimeras tested, PtmO5-RhFRed, generated by linking PtmO5 with the reductase domain of $P450_{RhF}$,[28] provided the most promising outcome in the hydroxylation of **9** and **13.** Further co-expression of PtmO5-RhFRed, GroES/EL chaperone and the phosphite dehydrogenase Opt13 for NADPH regeneration in a single *E. coli* C41(DE3) strain allowed selective C11 hydroxylation of **13** to be attained with 88% isolated yield on preparative scale.

Variants of $P450_{BM3}$ have proven to be highly effective biocatalysts for selective oxidations of readily available terpene scaffolds,[31] including the A ring oxidation of decalin-containing terpenes.[32] Based on these precedents, we postulated that some of these variants would be capable of performing similar oxidation on **9** or **13**. To test this hypothesis, we conducted preliminary screening of $P450_{BM3}$ alanine-scanning variants in our enzyme library[32] for the hydroxylation of **9** or **13**. While no hydroxylation activity could be observed with **9**, we were delighted to observe the formation of oxidized product(s) from **13** with some of the variants tested. Variant BM3 MERO1 M177A in particular produced the C2-hydroxylated product **22** selectively without any over-oxidation or formation of C16–C17 epoxide side product. These results demonstrate the ready tunability of these oxidation biocatalysts to achieve selective reaction in the presence of other reactive functional group(s), a notable advantage over chemical oxidation methods. Importantly, this serendipitous discovery identified a solution for the A ring oxidation problem.

Chemoenzymatic synthesis of oxidized *ent*-kauranes

While the full substrate scope profile of the three enzymes above were unclear at the outset of this work, the promiscuity of many other bacterial oxygenases[21,33] prompted us to make a strategic bet that they would be promiscuous enough for divergent synthesis. Three *ent*-kauranes that would require the use of only remote B ring oxidation were initially targeted (Figure 3), namely mitrekaurenone (**25**), fujenoic acid (**27**), and pharboside aglycone (**29**). These three molecules contain different oxidation states and stereochemical configurations at C6 and C7, and their divergent synthesis would provide an ideal testbed for the synthetic versatility of biocatalytic oxidation with PtmO6. Steviol (**9**) was first converted to *ent*-kaurenoic acid (**13**) via a two-step protocol involving brominative displacement of the 3º alcohol and radical dehalogenation. The use of PtmO6 on **13** allowed selective installation of a 2º alcohol at C7, delivering the product as a single diastereomer with good conversion and yield. This transformation could be carried out routinely on gram scale using clarified lysate of *E. coli* cells expressing PtmO6. Conversion of alcohol **18** to the corresponding ketone (**24**) was accomplished by treatment with DMP. Introduction of the C6 α-OH of mitrekaurenone would require oxidation from the more hindered face of the skeleton. Thus, a strategy featuring an S_N2-type displacement of a β-disposed leaving group at C6 by the C19 acid was pursued. Gratifyingly, α-oxidation with pyridinium tribromide was found to elicit simultaneous intramolecular lactonization by the C19 acid, thereby completing the synthesis of mitrekaurenone in five steps.

To access fujenoic acid (**27**), a net ten electron oxidation needed to be carried out on the B ring of the scaffold. Chemical methods for α-hydroxy ketone synthesis were initially attempted on **24** but we fortuitously found that PtmO6 is capable of installing the C6 alcohol with superior yield. Oxidative cleavage of the C6–C7 bond with $NaIO_4$, followed by hemiketal oxidation with DMP furnished fujenoic acid (**27**) in seven steps from **9**. Pharboside aglycone (**29**), on the other hand, contains a β-disposed *syn*-diol motif at C6 and C7. While **26** could potentially be a viable synthetic intermediate, the conversion of its α-hydroxy ketone functionality to the desired diol motif would require a difficult reduction from the more hindered face. As an alternative, the 2º alcohol of methyl ester **28** was dehydrated to the corresponding olefin with Burgess reagent, thereby allowing the C6,C7 *syn*-diol motif to be introduced via dihydroxylation. The use of OsO_4 and NMO simultaneously converted the two olefins to the corresponding *syn*-diol units and completed the synthesis of **29** in six steps from steviol.

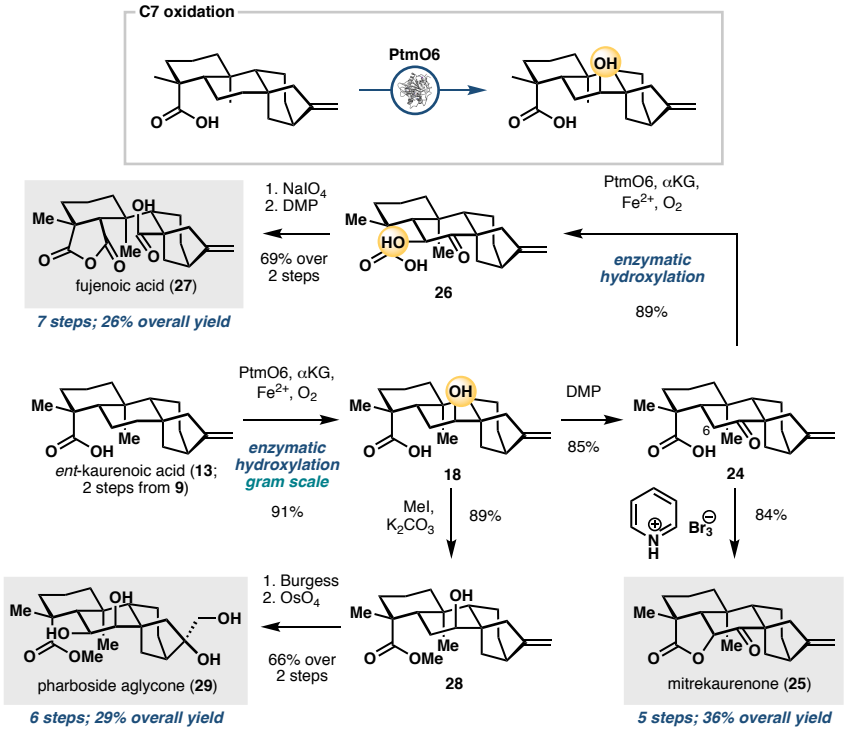

Figure 3. Application of PtmO6 in the chemoenzymatic total synthesis of mitrekaurenone (**25**), fujenoic acid (**27**) and pharboside aglycone (**29**).

Next, we sought to demonstrate the utility of our strategy in the preparation of *ent*-kauranes that contain oxidations on multiple rings (Figure 4), such as rosthornins B (**3**) and C (**34**), and fischericin B (**2**). These targets were chosen to highlight how multiple enzymatic hydroxylation reactions could be combined together or used strategically in combination with the concept of innate and guided C–H functionalization logic.[19] Access to **3** and **34** from steviol would require hydroxylation at C7 and C11 with PtmO6 and PtmO5-RhFRed, reduction of the carboxylic acid at C19, and introduction of a carbonyl group at C15. To install the two alcohols at C7 and C11, a strategic decision had to be made in terms of the ordering of the two enzymatic hydroxylation steps. Performing C11 hydroxylation prior to C7 hydroxylation would necessitate nontrivial differentiation between the two alcohols for subsequent acetylation at C11 and stereochemical inversion at C7. Conversely, oxidation at C7 prior to that at C11 would allow the use of a carbonyl

motif at C7 as a 'masking' group for the C7 α-OH and minimize potential chemoselectivity issues in subsequent manipulations, though the success of this sequence would hinge on the ability of PtmO5-RhFRed to accept a non-native substrate. As this hypothesis could easily be tested within two steps into the synthesis, the latter route was pursued. Gratifyingly, ketone **30**, accessed in two steps from **9** via PtmO6 hydroxylation and DMP oxidation, could undergo a regioselective hydroxylation at C11 with PtmO5-RhFRed, albeit with only moderate conversion. Using lysates of *E. coli* expressing PtmO5-RHFRed and Opt13, C11 hydroxylation of **30** could be carried out with 65% isolated yield. The use of Ac_2O and catalytic DMAP allowed selective acetylation of the C11 alcohol without any undesired side reaction with the 3º alcohol at C13. At this stage, the C19 carboxylic acid needed to be reduced to the alcohol without concomitant removal of the acetate group at C11. This was achieved by first converting the acid to the corresponding acyl imidazole (**32**), followed by treatment with $NaBH_4$, which also led to concomitant reduction of the C7 ketone to the α-disposed alcohol. Installation of the enone unit on the D ring via selective C15–OH oxidation with SeO_2 and IBX completed the synthesis of rosthornin C (**34**) in seven steps overall. Finally, conversion of **34** to rosthornin B (**3**) could be effected via selective acetylation of the primary alcohol at C19.

Fischericin B (**2**) contains a caged ether motif that is reminiscent of platensimycin and a bridging lactone ring between C19 and C20. Synthesis of **2** would thus provide an opportunity to develop a hybrid strategy that combines enzymatic hydroxylation at C11 and alkoxy-radical-based C–H functionalization at C20. Our synthesis commenced with PtmO5-catalyzed C11 hydroxylation of **9**. Using information gleaned from prior biosynthetic studies of platensimycin,[26] the hydroxylated product could be treated with strong acidic conditions to construct the desired caged ether motif. In the presence of this motif, the C13 tertiary alcohol proved inert to conversion to the corresponding bromide for subsequent radical debromination. As a workaround, the free acid of **35** was first methylated and a Barton deoxygenation was performed on its C13 tertiary alcohol. The key hypoiodite–mediated C20 functionalization under Suarez conditions[17,34] cleanly delivered iodoaldehyde **39**, which could be further oxidized and subjected to intramolecular ring closure to complete our synthesis of fischericin B (**2**) in just nine steps.

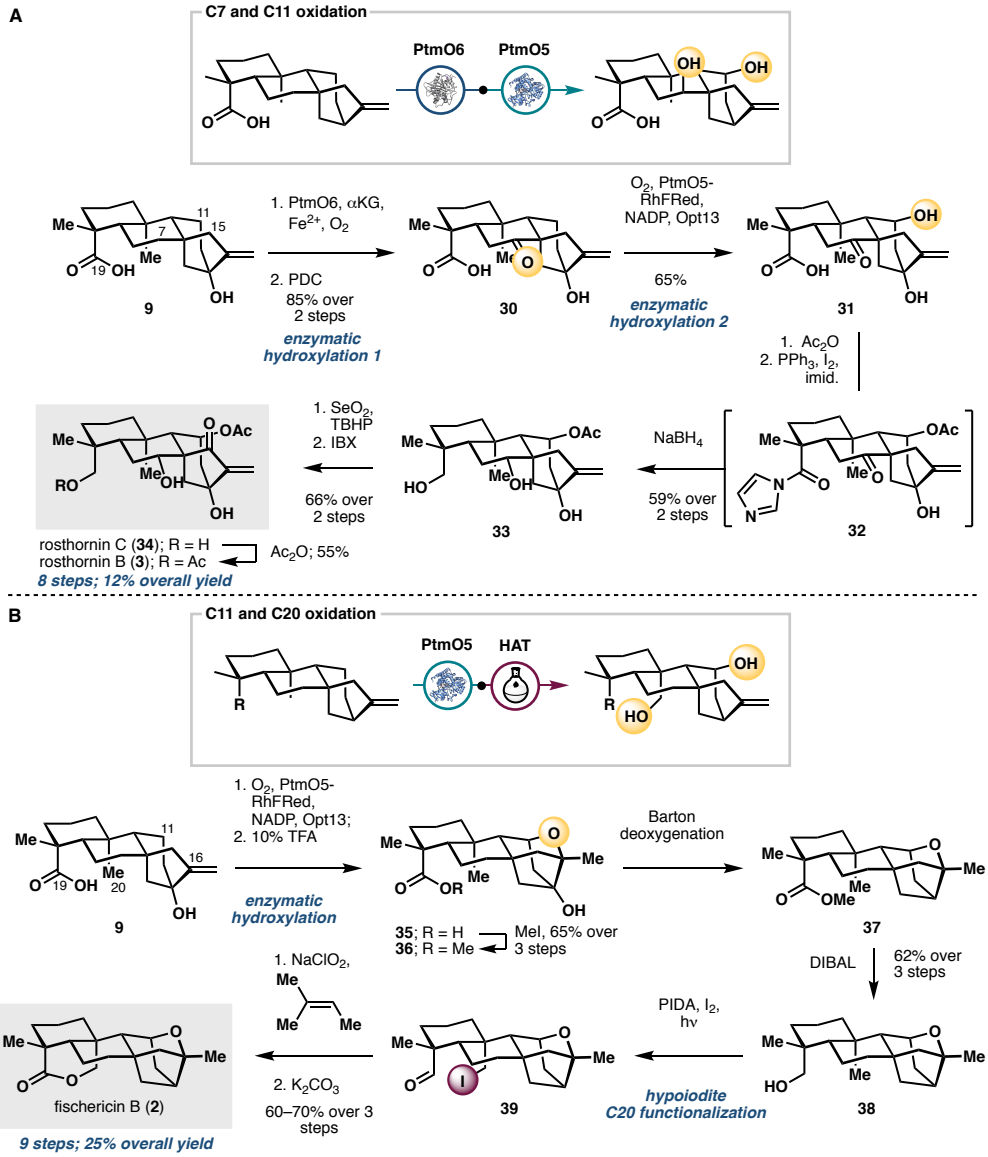

Figure 4. Application of PtmO5-RhFRed in the chemoenzymatic total synthesis of rosthornins B (**3**) and C (**34**) and fischericin B (**2**).

Oxidation-enabled skeletal rearrangement to *ent*-atisane and *ent*-trachylobane

Access to minimally oxidized *ent*-atisane and *ent*-trachylobane skeletons commenced from isosteviol (**40**), an *ent*-beyerane available in one step via acid-catalyzed degradation/rearrangement of stevioside (Figure 5A). Execution of our synthetic blueprint required the installation of a functional group at C12 that is suited for subsequent carbocation generation. We envisioned first C11 hydroxylation of **40** with PtmO5-RhFRed, followed by a C11 to C12 transposition of the resulting alcohol. Hydroxylation of isosteviol with PtmO5-RhFRed unexpectedly proceeded at its C12 carbon instead of C11, thereby obviating the need for any further functional group interconversions. Furthermore, this reaction proceeded with high conversion and yield, and could be carried out routinely on multi-gram scale in a single pass. The unexpected switch in regioselectivity could be rationalized by the difference in C ring conformation of *ent*-kaurane and *ent*-beyerane. PtmO5 oxidizes the axial C11 β-H of its native substrate. In contrast, the equivalent

C11 β-H on **40** adopts an equatorial configuration, and is therefore inaccessible for abstraction by the active Fe(IV)-oxo species. Instead, C–H abstraction takes place at the adjacent axial C12 β-H. Treatment of **41** with TfOH initiated the intended Wagner–Meerwein rearrangement, delivering **42**, which contains the requisite *ent*-atisane [2.2.2] C/D ring bicycle. Access to *ent*-trachylobane skeleton from **42** required the formation of a new C–C bond between C13 and C16. Examination of several different methods[35] to forge this bond led to the discovery of a reductive rearrangement in the presence of BF_3•Et_2O and Et_3SiH, which afforded an *ent*-trachylobane product **44** from **43** in 61% yield after 3x recycling. We propose that this rearrangement proceeds via ionization of C13 alcohol, followed by formation of a non-classical carbocation and selective reductive quenching at C15. Overall, this synthetic sequence provides rapid and controlled access to *ent*-atisane and *ent*-trachylobane frameworks from isosteviol in two and four steps respectively and is only made possible by the serendipitous discovery of PtmO5-catalyzed C12 hydroxylation of **40**.

Preliminary investigation suggests that **42** is a useful intermediate for accessing more oxidized *ent*-atisanes via enzymatic hydroxylation (Figure 5B). It bears high structural resemblance to the native *ent*-atiserenoic acid precursor of plantensin.[9,27] Unsurprisingly, it is capable of undergoing oxidation at C7 with PtmO6. Notably, **42** could be hydroxylated by PtmO6 in a more efficient fashion than its C13-deoxy counterpart. Wolff–Kishner deoxygenation of C13 ketone and PDC oxidation of C7-OH afforded ketone **46**, which represents a potential intermediate towards spiramilactone C (**5**). In an alternative sequence, **42** could first be oxidized at C2 with BM3 MERO1 M177A to acid **47** without any observable epoxidation of its C15–C16 olefin. Wolff–Kishner reduction delivered **48**, which possesses the appropriate functionalities to be converted to the diterpenoid alkaloid cochleareine (**6**).

Chemoenzymatic synthesis of the mitrephorones

Intermediate **44** could be used to divergently prepare mitrephorones A, B and C (**7**, **53**, **8**, Figure 5C). We hypothesized that **44** possesses high enough structural similarity to **9** or **13** to be accepted as substrates by BM3 MERO1 M177A and PtmO6. Gratifyingly, C2 oxidation of **44** with BM3 MERO1 M177A was found to proceed very efficiently. At high enough enzyme-to-substrate ratio, this process also led to iterative oxidation to install a ketone moiety at C2. Subjection of this compound to enzymatic oxidation with PtmO6, followed by PDC oxidation, furnished diketone **49**. Similar to our synthesis of fujenoic acid, PtmO6 was found to be capable of installing C6-OH on **49**. Completion of our synthesis of mitrephorone C (**8**) was achieved by methylation of the C19 acid with CH_2N_2, and further oxidation at C6 with DMP, followed by keto-enol tautomerization. Notably, **50** proved to be rather unstable, necessitating the use of conditions that allowed rapid methylation of the C19 acid and mild oxidation at C6.

Our foray to mitrephorone B (**52**) from **44** commenced via C7 enzymatic oxidation with PtmO6. Initial attempts focused on the dehydration of the C7-OH to the corresponding olefin, followed by a ruthenium-catalyzed direct oxidation (*36*) to install the C6–C7 dione moiety. Unfortunately, this sequence was found to be low yielding and accompanied by significant amounts of side-product even at low conversion. It is also worth noting that this sequence provided no desired product at all when the C2 carbon exists in the ketone oxidation state (i.e., for the mitrephorone C series). As a workaround, **44** was oxidized to the corresponding ketone (**52**), which was submitted to enzymatic hydroxylation at C6 with PtmO6, followed by methylation and oxidation with PDC. While this route led to one more step than the dehydration/oxidation sequence, it provided a superior overall yield and was thus preferred. According to Magauer's report,[12] conversion of **53** to mitrephorone A (**7**) could be achieved through the use of

electrochemical oxidation or White's Fe(PDP) catalyst. We found serendipitously that **52** is capable of undergoing a slow autoxidation to form **7** (45% yield after 7 days, or 65% yield after 14 days). Such autoxidation did not take place with **8**, suggesting that distal substituents are capable of modulating the reactivity of the diosphenol motif of **53**. This discovery allowed us to divergently prepare the entire known family members of the mitrephorones from **44**. Notably, the use of enzymatic oxidations with PtmO5-RhFRed, PtmO6 and BM3 MERO1 M177A proved to be highly enabling as all three members of the family could be prepared in less than ten steps, a marked improvement over previous routes to the mitrephorones.[11,12]

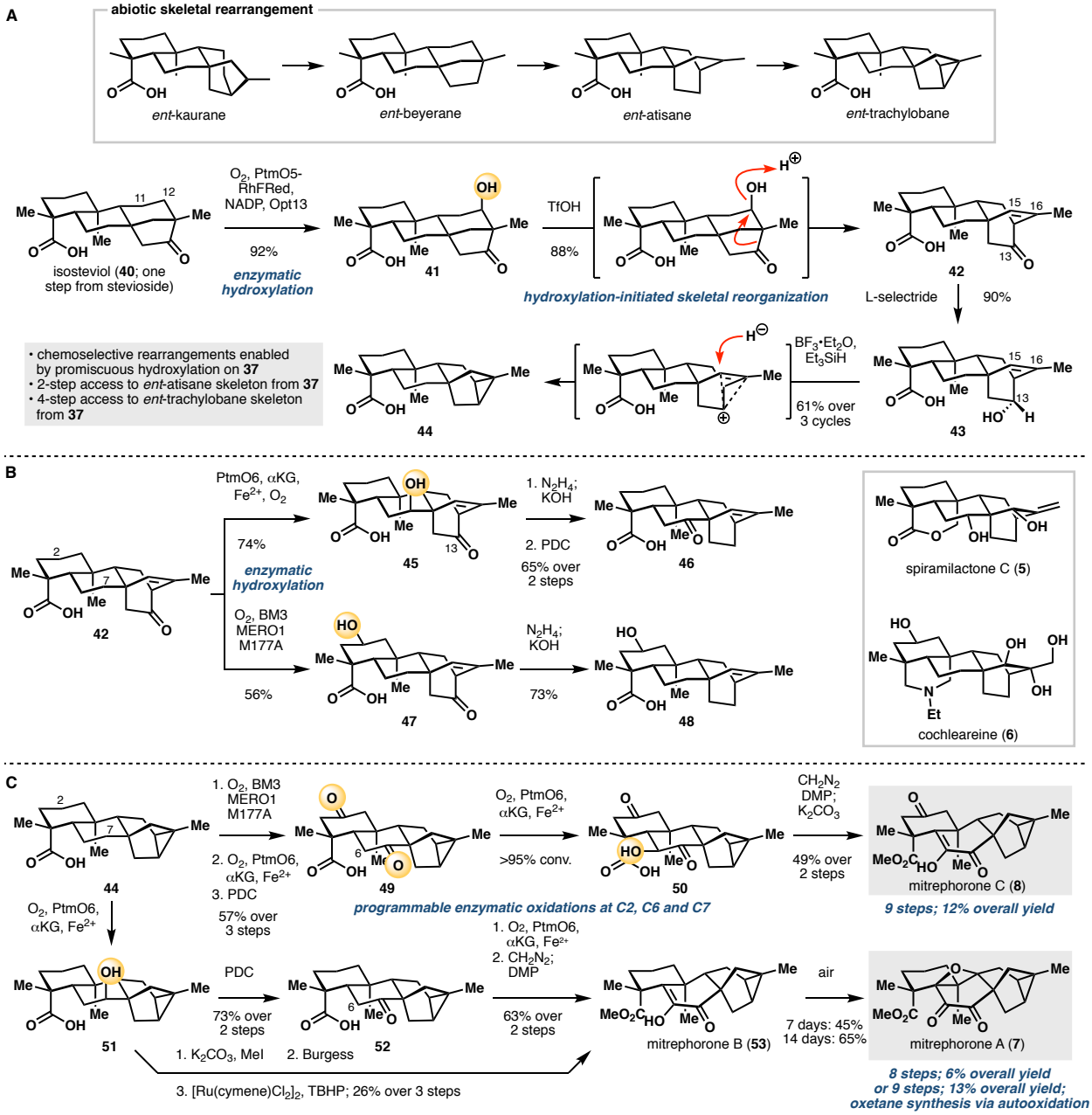

Figure 5. A. Conversion of isosteviol (**40**) to *ent*-atisane and *ent*-trachylobane products via site-selective C12 hydroxylation and carbocationic rearrangements. **B.** Further site-selective oxidations of **42** using PtmO6 and BM3 MERO1 M177A. **C.** Divergent chemoenzymatic total synthesis of the mitrephorones starting from **44**.

Conclusion

The chemoenzymatic strategy presented in this work resulted in the preparation of nine highly oxidized *ent*-kaurane and *ent*-trachylobane natural products in less than ten steps each. Central to this strategy is the identification of three selective and scalable biocatalytic processes that are able to hydroxylate the A, B and C rings of the parent carbocyclic structures with site-selectivity and functional group compatibility unmatched by any known small-molecule reagents or catalysts. Further leveraging of the newly-introduced hydroxyl groups in a series of carbocationic rearrangements enables rapid traversal of the diterpene landscape spanning the *ent*-kaurane, *ent*-atisane and *ent*-trachylobane families. By virtue of the substrate promiscuity of the enzymes, the biocatalytic oxidations can also be carefully permuted and used in conjunction with chemical C–H oxidations in multi-step synthetic sequences for streamlined access to complex natural products with minimal functional group interconversions and protecting group manipulations.[37] In the context of synthetic strategy development, this work addresses many of the limitations of the recently-developed 'two-phase' strategy for terpene synthesis,[38] which at times requires circuitous oxidative transformations due to its sole reliance on small-molecule reagents or catalysts. The marriage of chemical and enzymatic C–H oxidations, in particular, constitutes a powerful means to streamline access to highly oxidized terpenes. The strategy outlined here opens the door for rapid synthetic access to a wide array of natural and unnatural *ent*-kauranes, *ent*-atisanes and *ent*-trachylobanes and in light of their intriguing biological activities, future efforts in this arena will facilitate the design of novel ligands and chemical probes for biological discovery.[39]

References and Notes:

1. Liu, M.; Wang, W.-G.; Sun, H.-D.; Pu, J.-X. *Nat. Prod. Rep.* **2017**, *34*, 1090.
2. Liao, Y.-J.; Bai, H.-Y.; Li, Z.-H.; Zou, J.; Chen, J.-W.; Zheng, F.; Zhang, J.-X.; Mai, S.-J.; Zeng, M.-S. Sun, H.-D.; Pu, J.-X.; Xie, D. *Cell Death Dis.* **2014**, *5*, e1137.
3. Li, D.; Li, C.; Li, L.; Chen, S.; Wang, L.; Qi, L.; Wang, X.; Lei, X.; Shen, Z. *Cell Chem. Biol.* **2016**, *23*, 257.
4. He, H.; Jiang, H.; Chen, Y.; Ye, J.; Wang, A.; Wang, C.; Liu, Q.; Liang, G.; Deng, X.; Jiang, W.; Zhou, R. *Nat. Commun.* **2018**, *9*, 2550.
5. Friese, J.; Gleitz, J.; Guster, U. T.; Heubach, J. F.; Matthiesen, T.; Wilffert, B.; Selve, N. *Eur. J. Pharmacol.* **1997**, *337*, 165.
6. Wang, W.; Liu, H.; Wang, S.; Hao, X.; Li, L. *Cell Res.* **2011**, *21*, 730.
7. Li, C.; Lee, D.; Graf, T. N.; Phifer, S. S.; Nakanishi, Y.; Burgess, J. P.; Riswan, S.; Setyowati, F. M.; Saribi, A. M.; Soejarto, D. D.; Farnsworth, N. R.; Falkinham, J. O. 3rd, Kroll, D. J.; Kinghorn, A. D.; Wani, M. C.; Oberlies, N. H. *Org. Lett.* **2005**, *7*, 5709.
8. Hong, Y. J.; Tantillo, D. J. *J. Am. Chem. Soc.* **2010**, *132*, 5375.
9. Smanski, M. J.; Yu, Z.; Casper, J.; Lin, S.; Peterson, R. M.; Chen, Y.; Wendt-Pienkowski, E.; Rajski, S. R.; Shen, B. *Proc. Natl. Acad. Sci. USA* **2011**, *108*, 13498.
10. Yeoman, J. T. S.; Mak, V. W.; Reisman, S. E. *J. Am. Chem. Soc.* **2013**, *135*, 11764.
11. Richter, M. J. R.; Schneider, M.; Brandstätter, Krautwald, S.; Carreira, E. M. *J. Am. Chem. Soc.* **2018**, *140*, 16704.
12. Wein, L. A.; Wurst, K.; Angyal, P.; Weisheit, L.; Magauer, T. *J. Am. Chem. Soc.* **2019**, *141*, 19589.
13. Kou, K. G. M.; Kulyk, S.; Marth, C. J.; Doering, N. A.; Li, B. X.; Gallego, G. M.; Lebold, T. P.; Sarpong, R. *J. Am. Chem. Soc.* **2017**, *139*, 13882.

14. Zhao, X.; Li, W.; Wang, J.; Ma, D. *J. Am. Chem. Soc.* **2017**, *139*, 2932.
15. Kenny, M. J.; Mander, L. N.; Sethi, S. P. *Tetrahedron Lett.* **1986**, *27*, 3927.
16. Cherney, E. C.; Lopchuk, J. M.; Green, J. C.; Baran, P. S. *J. Am. Chem. Soc.* **2014**, *136*, 12592.
17. Kobayashi, S.; Shibukawa, K.; Hamada, Y.; Kuruma, T.; Kawabata, A.; Masuyama, A. *J. Org. Chem.* **2018**, *83*, 1606.
18. Kawamata, Y.; Yan, M.; Liu, Z.; Bao, D.-H.; Chen, J.; Starr, J. T.; Baran, P. S. *J. Am. Chem. Soc.* **2017**, *139*, 7448.
19. Brückl, T.; Baxter, R. D.; Ishihara, Y.; Baran, P. S. *Acc. Chem. Res.* **2012**, *45*, 826.
20. Hung, K.; Condakes, M. L.; Novaes, L. F. T.; Harwood, S. J.; Morikawa, T.; Yang, Z.; Maimone, T. J. *J. Am. Chem. Soc.* **2019**, *141*, 3083.
21. Lowell, A. N.; Demars, M. D., II; Slocum, S. T.; Yu, F.; Anand, K.; Chemler, J. A.; Koravaki, N.; Priessnitz, J. K.; Park, S. R.; Koch, A. A.; Schultz, P. J.; Sherman, D. H. *J. Am. Chem. Soc.* **2017**, *139*, 7913.
22. Xu, G.; Elkin, M.; Tantillo, D. J.; Newhouse, T. R.; Maimone, T. J. *Angew. Chem. Int. Ed.* **2017**, *56*, 12498.
23. Hellwell, C. A.; Chandler, P. M.; Poole, A.; Dennis, E. S.; Peacock, W. J. *Proc. Natl. Acad. Sci. USA* **2001**, *98*, 2065.
24. Nett, R. S.; Montaranes, M.; Marcassa, A.; Lu, X.; Nagel, T. C.; Charles, P.; Hedden, P.; Rojas, M. C.; Peters, R. J. *Nat. Chem. Biol.* **2017**, *13*, 69.
25. Takahashi, J. A.; Gomes, D. C.; Lyra, F. H.; dos Santos, G. F.; Martins, L. R. *Molecules* **2014**, *19*, 1856.
26. Rudolf, J. D.; Dong, L.-B.; Zhang, X.; Renata, H.; Shen, B. *J. Am. Chem. Soc.* **2018**, *140*, 12349.
27. Dong, L.-B.; Zhang, X.; Rudolf, J. D.; Deng, M.-R.; Kalkreuter, E.; Cepeda, A. J.; Renata, H.; Shen, B. *J. Am. Chem. Soc.* **2019**, *141*, 4043.
28. Li, S.; Podust, L. M.; Sherman, D. H. *J. Am. Chem. Soc.* **2007**, *129*, 12940.
29. Lu, C.; Shen, F.; Wang, S.; Wang, Y.; Liu, J.; Bai, W.-J.; Wang, X. *ACS Catal.* **2018**, *8*, 5794.
30. Sibbesen, O.; De Voss, J. J.; Ortiz de Montellano, P. R. *J. Biol. Chem.* **1996**, *271*, 22462.
31. Whitehouse, C. J. C.; Bell, S. G.; Wong, L.-L. *Chem. Soc. Rev.* **2012**, *41*, 1218.
32. Li, J.; Li, F.; King-Smith, E.; Renata, H. *Nat. Chem.* **2020**, *12*, 173.
33. Schmidt, J. J.; Khatri, Y.; Brody, S. I.; Zhu, C.; Pietraszkiewicz, H.; Valeriote, F. A.; Sherman, D. H. *ACS Chem. Biol.* **2020**, *15*, 524.
34. Yu, W.; Hjerrild, P.; Overgaard, J.; Poulsen, T. B. *Angew. Chem. Int. Ed.* **2016**, *55*, 8294.
35. Kelly, R. B.; Beckett, B. A.; Eber, J.; Hung, H.-K.; Zamecnik, J. *Can. J. Chem.* **1975**, *53*, 143.
36. Kawamura, S.; Chu, H.; Felding, J.; Baran, P. S. *Nature* **2016**, *532*, 90.
37. Gaich, T.; Baran, P. S. *J. Org. Chem.* **2010**, *75*, 4657.
38. Yuan, C.; Jin, Y.; Wilde, N. C.; Baran, P. S. *Angew. Chem. Int. Ed.* **2016**, *55*, 8280.
39. S. L. Schreiber *et al. Cell* **2015**, *161*, 1252.

Acknowledgments: We thank Profs. Phil S. Baran, Ryan A. Shenvi, Thomas J. Maimone and Keary M. Engle for useful discussions. **Funding:** This work is supported, in part, by the National Institutes of Health Grant GM134954 (B.S.), GM128895 (H.R.) and GM124461 (J.D.R.).

Author contributions: X.Z. and H.R. conceived of the work. X.Z., E.K.-S., L.-B.D., L.-C.Y., and J.D.R. designed and executed experiments. B.S. and H.R. provided insight and direction for experimental design.

Competing interests: Authors declare no competing interests.

Data and materials availability: All data is available in the main text or the supplementary materials.

Supplementary Materials:

Materials and Methods

Figures S1, S2

Tables S1–S19

References (*1–46*)